Research article

Dev Reprod 2024;28(3):67-74
https://doi.org/10.12717/DR.2024.28.3.67

Development & Reproduction

ISSN 2465-9525 (Print)
ISSN 2465-9541 (Online)

Autotaxin Expression in the Uterus of Cycling Rats

Hye-Soo Kim, †Sung-Ho Lee

Department of Biotechnology, Sangmyung University, Seoul 03016, Korea

Received: June 17, 2024
Revised: August 25, 2024
Accepted: September 8, 2024

†Corresponding author
Sung-Ho Lee
Department of Biotechnology, Sangmyung University, Seoul 03016, Korea.
Tel: +82-2-2287-5139
E-mail: shlee@smu.ac.kr

ORCID
Hye-Soo Kim
https://orcid.org/0009-0009-1331-167X
Sung-Ho Lee
https://orcid.org/0000-0003-2866-3642

Conflict of interests
The authors declare no potential conflict of interest.

Acknowledgements
Not applicable.

Authors' contributions
Conceptualization: Lee SH.
Data curation: Lee SH.
Formal analysis: Lee SH.
Methodology: Kim HS, Lee SH.
Validation: Lee SH.
Investigation: Kim HS, Lee SH.
Writing-original draft: Lee SH.
Writing-review & editing: Kim HS, Lee SH.

Ethics approval
All animal experiments were conducted in accordance with the Guide for the Care and Use of Laboratory Animals published by the National Institute of Health (approval number R-2301-1).

Abstract

Autotaxin (ATX), also known as ectonucleotide pyrophosphatase/phosphodiesterase family member 2 (ENPP 2), is an enzyme with lysophospholipase D activity that converts lysophosphatidylcholine into lysophosphatidic acid (LPA). One of the LPA receptors, LPA3, is positively and negatively regulated by progesterone and estrogen, respectively. Furthermore, ATX expression in the rat uterus could be under the control of estrous cycle. In the present study, we used young normal cycling rats for further assess the uterine ATX expression and localization by reverse transcription PCR (RT-PCR) and immunohistochemistry, respectively. In the RT-PCR study, ATX mRNA level at Metestrus (1.00±0.026 AU) was significantly higher than that at Proestrus (0.42±0.046 AU, $p<0.001$) and the level at Diestrus (0.75±0.107 AU, $p<0.05$) was significantly higher than that at Proestrus. Among the luminal epithelial cells, the order of the ATX signal intensities was Metestrus>Diestrus>Proestrus>Estrus. Among the myometrial cells, the order of the signal intensities was Diestrus>Proestrus>Estrus>Metestrus. Among the glandular epithelial cells, the order of the signal intensities was Proestrus>Estrus=Metestrus=Estrus. The present study indicates that expression and localization of uterine ATX may be under the control of sex steroids during the estrous cycle. Further studies on the ATX signaling–sex steroid relationship will be providing better understanding on in normal and pathophysiological state of uterus.

Keywords: Autotaxin (ATX), Lysophosphatidic acid (LPA), Estrous cycle, Reverse transcription-PCRs (RT-PCRs), Immunohistochemistry, Sex steroids

INTRODUCTION

Autotaxin (ATX), also known as ectonucleotide pyrophosphatase/phosphodiesterase family member 2 (ENPP 2), is an enzyme that in humans is encoded by the ENPP2 gene (Kawagoe et al., 1995). ATX is an extracellular hydrolase which has lysophospholipase D activity that converts lysophosphatidylcholine (LPC) into lysophosphatidic acid (LPA), a lipid signaling molecule (Hausmann et al., 2013). The binding of LPA to its receptors (LPAR1-6s) activates multiple cellular signaling pathways resulting various physiological changes (Yang & Chen, 2018).

ATX was originally identified as a tumor cell-motility-stimulating factor; later it was shown to be LPA which is responsible for its effects on cell-proliferation (Umezu-Goto et al., 2002; Nakanaga et al., 2010; Brindley, 2020). Indeed, ATX signaling is deeply involved in the proliferation and metastasis of breast cancer, prostate cancer, endometrial cancer, and ovarian cancer cells (Nouh et al., 2009; Zeng et al., 2009; Benesch et al., 2014; Mazzocca et al., 2018; Drosouni et al., 2022; Choi et al., 2023).

In mice, ATX expression has been confirmed from embryonic period to adult, and the expression is temporally and spatially regulated (Zhang et al., 2021). In adult mice, adipose tissue, central nervous system, placenta, and lymph nodes have the highest expression levels of ATX (Kanda et al., 2008; Katsifa et al., 2015). In mouse uterus, one of the LPA receptors, LPA3, is positively and negatively regulated by progesterone and estrogen, respectively (Hama et al., 2006). Additionally, ATX is expressed in the rat uterus, and this could be under the control of estrous cycle (Ahn et al., 2011). These studies strongly suggest the possibility that ATX-LPA-LPAR signaling might functions in the uterus, where cell division/death is actively occurred, but there has been no progress in related research. In the present study, we used young normal cycling rats for further assess the uterine ATX expression and localization by reverse transcription RT-PCR and immunohistochemistry, respectively.

MATERIALS AND METHODS

1. Animals

Young female rats (about 10 weeks old, Sprague-Dawley strain) were provided by DBL (Eumseong, Korea) and reared in Sangmyung university animal facility under photoperiods of 12 h light/dark with lights on at 0700 hr and constant temperature of 21℃–23℃. Food and tap water were supplied *ad libitum*. The animal protocols were approved by the Animal Care and Use Committees at Sangmyung university (approval number R-2301-1). All the animals received humane care in accordance with the guides for animal experiments of the Association for Assessment and Accreditation of Laboratory Animal Care (AAALAC).

2. Estrous cycle check and tissue collection

After 2 weeks of acclimation, vaginal smears were collected daily (between 0900 and 1000 hr) for three consecutive cycles, and only rats which showed regular 4-day estrous cycles were used for this study. Five animals of each estrous stage were sacrificed by decapitation between 1800 and 1830 hr. Immediately, ovaries and uteri were collected for RT-PCR and immunohistochemistry.

3. Total RNA isolation

The tissues were immediately soaked in the RNA isolation solution, stored at −70℃ until RT-PCRs. Total RNAs were isolated from samples using the acid guanidinium thiocyanate-phenol-chloroform (AGPC) procedure. To five volumes of the RNA extraction solution containing the sample were added 1 volume of 3 M sodium acetate (pH 5.2, Bioneer, Daejeon, Korea) and 6 volumes of PCI (pH 4.3, 5:1 Phenol:Chloroform, Bioneer) in a 1.5 mL tube (Hankuk Bioscience, Seongnam, Korea). Mixed samples by inverting were centrifuged at 14,000×g for 25 min in cooling centrifuge (Hanil, Gimpo, Korea) at 4℃. The supernatant was carefully transferred to a new tube and the same volume of isopropanol (Duksan, Ansan, Korea) was added. The samples were mixed and placed over an hour at −20℃. The samples were centrifuged prior to the supernatant removed. The precipitated pellet was added to the RNA extraction solution and this process was repeated once more. Then the RNA pellet was washed with 1 mL of 70% ethanol (Merck, Darmstadt, Germany) twice by centrifugation. The final pellet was resuspended in diethylpyrocarbonate (DEPC; Sigma-Aldrich, St. Louis, MO, USA)-treated distilled water. The samples were stored at −70℃ before using.

4. Reverse transcription-PCRs (RT-PCRs)

Total RNAs were used in RT-PCR reactions carried out with Maxime™ RT PreMix (InTron,

https://doi.org/10.12717/DR.2024.28.3.67

Seongnam, Korea) and AccuPower PCR Premix (GeneAll, Seoul, Korea) according to the manufacturer's instructions. Sequences of the primers and the specific PCR conditions used in this study were listed in Tables 1 and 2, respectively. The reactions were subjected to MultiGene™ OptiMax Thermal Cycler (Labnet, Edison, NJ, USA). The reaction products were analyzed by gel electrophoresis in 1.5% agarose gel (75 V, 65 min) and visualized by ethidium bromide staining (Dye All, GeneAll). The band intensities were measured using the image analysis system (Imager Ⅲ-1D main software, Bioneer). Glyceraldehydes-3-phosphate dehydrogenase (GAPDH) was used as reference gene for normalization of quantitative RT-PCRs in the present study.

5. Paraffin tissue section

Fixed uteri were dehydrated in graded concentrations of ethanol (70%, 80%, 90%, 95%, and 100%; Duksan) for 1 h 30 min in each with gentle shaking and soaked in absolute ethanol overnight. The tissues were immersed in xylene (Samchun Chemical, Seoul, Korea) for 30 min, 3 times and in paraffin at 56℃ for 30 min, 3 times. The tissues were embedded in paraffin and sectioned (Microm, Walldrof, Germany) at 5 μm. The samples were attached on microscope slides and the slides were stained with hematoxylin (Sigma-Aldrich) for 5 min and eosin (Across, Carson, CA, USA) for 5 min, respectively.

6. Immunohistochemistry

The slides were dewaxed in xylene for 5 min, 3 times and hydrated in 100%, 95%, 90%, 80%, and 70% ethanol for 5 min each. The specimens were washed in phosphate buffered saline (PBS) for 5 min, 4 times and immersed in hydrogen peroxide solution [10% H_2O_2 (Daejung, Siheung, Korea) and 10% Methanol (Merck)] in PBS for 20 min, and washed in PBS 2 times. The slides were incubated with blocking serum [2% BSA (BioPURE, Cambridge, MA, USA) and 2% normal goat serum (Vector, Road Burlingame, CA, USA)] in PBS for 1 h and incubated with diluted the primary antibody for ATX (1:80; item No. 10005375; Cayman, Ann Arbor, MI, USA) in blocking serum overnight. And then, the slides were washed 2 times and incubated with biotinylated goat anti-rabbit IgG secondary antibody (Vector) for 1 h and washed in PBS 2 times. The samples were incubated with avidin-biotin-peroxidase complex using the ABC kit (Vector) for 40 min and washed 2 times. The chromogenic reaction was progressed using the DAB kit (Vector) and stopped

Table 1. Accession numbers, primer sequences and product sizes used in this study

Gene	Accession number	Sequence of the primers	Product size (bp)
ATX	NM_181692.2	F 5'-CTG TGT TCG TCC TGA TGT CC	370
		R 5'-GCT GGT GAT GCT GTA GTA G	
GAPDH	NM_017008.4	F 5'-CCA TCA CCA TCT TCC AGG AG	576
		R 5'-CCT GCT TCA CCC ACC TTC TTG	

ATX, autotaxin; GAPDH, glyceraldehydes-3-phosphate dehydrogenase.

Table 2. PCR conditions used in this study

Gene	Temperature & time	Number of cycles
	denature / annealing / extension	
ATX	95℃, 35 sec / 54℃, 35 sec / 72℃, 45 sec	41
GAPDH	95℃, 60 sec / 55℃, 35 sec / 72℃, 60 sec	28

ATX, autotaxin; GAPDH, glyceraldehydes-3-phosphate dehydrogenase.

by washing in tap water. The slides were stained in hematoxylin (Sigma-Aldrich) for 7 min and dehydrated in graded ethanol (70%, 80%, 90%, 95%, and 100%) for 3 min each and then cleaned in xylene for 5 min, 3 times. The slides were mounted with Permount (Fisher Scientific, Waltham, MA, USA). The images were captured with the BX51 Microscope & DP70 Digital Camera System (Olympus, Tokyo, Japan).

7. Statistical analysis

All experiments were performed at least three times. Values were expressed as mean±SE. Data were analyzed using One-way analysis of variance (ANOVA) as indicated. $p<0.05$ was considered statistically significant. Calculations were performed using Graphpad Software Prism version 5.

RESULTS

1. Changes in tissue weights

To investigate the changes in the weight and ATX expression in rat uterus during the estrous cycle, uteri from each stage of the cycle were confirmed according to vaginal cytology. The uterine weight changes by stage during the estrous cycle are shown in Table 3. The order of the uterine weight is Diestrus<Metestrus<Estrus≤Proestrus; the weights between the Metestrus (394.02 ±90.99 mg, $p<0.01$) and Diestrus (454.72±50.63 mg, $p<0.01$) were significantly lower than the weight at Proestrus stage (571.34±56.64 mg). There was no significant difference between the uterine weights at Proestrus and Estrus (556.13±220.6 mg).

2. Changes in the uterine autotaxin (ATX) mRNA level during estrous cycle

In the RT-PCR study, ATX mRNA level at Metestrus (1.00±0.026 AU) was significantly higher than that at Proestrus (0.42±0.046 AU, $p<0.001$) and the level at Diestrus (0.75±0.107 AU, $p<0.05$) was significantly higher than that at Proestrus (Fig. 1).

3. Analysis of autotaxin (ATX) immunoreactivities during the estrous cycle

In general histology, the numbers of gland were increased at Metestrus and Diestrus. Fig. 2 represents the localization of the cells immunoreactive for ATX in cycling rat uteri. Among the luminal epithelial cells, the order of the ATX signal intensities was Metestrus>Diestrus>Proestrus>Estrus. Among the myometrial cells, the order of the signal intensities was Diestrus>Proestrus>Estrus>Metestrus. Among the glandular epithelial cells, the order of the signal intensities was Proestrus>Estrus=Metestrus=Diestrus.

DISCUSSION

ATX, a secreted glycoprotein enzyme, was first detected in conditioned medium of human A2058 melanoma cells as an autocrine motility factor (Stracke et al., 1992). ATX has lysophospholipase D activity, with its primary function being the extracellular hydrolysis of LPC to

Table 3. Changes in tissue weights during the rat estrous cycle

	Metestrus	Diestrus	Proestrus	Estrus
Ovary (mg)	49.8±11.57*	52.78±14.98	45.12±6.11**	62.43±13.65
Uterus (mg)	394.02±90.99##	454.72±50.63##	571.34±56.64	556.13±220.6

* $p<0.05$ versus Estrus; ** $p<0.01$ versus Estrus; ## $p<0.01$ versus Proestrus.

https://doi.org/10.12717/DR.2024.28.3.67

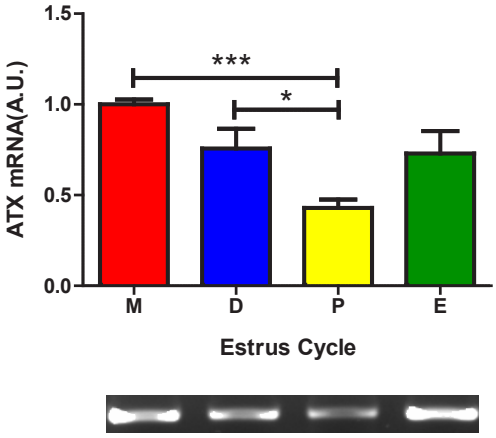

Fig. 1. Changes in uterine ATX mRNA levels during the rat estrous cycle. Young female rats which showed regular 4-day estrous cycles were used in this study. The primers and RT-PCR conditions were listed in Tables 1 and 2. The gel photograph under the graph is a representative of PCR reactions (n=5–6). * p<0.05, *** p<0.001. M, Mestrus; D, Diestrus; P, Proestrus; E, Estrus; A.U., arbitrary unit; ATX, autotaxin; RT-PCR, reverse transcription PCR.

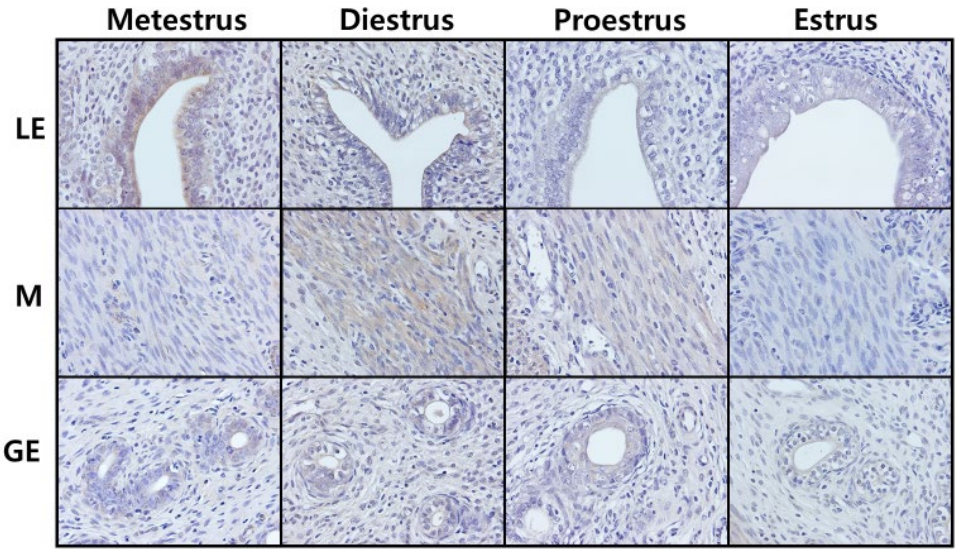

Fig. 2. Localization of ATX immunoreactivities in the uteri of cycling rat. The paraffin tissue section and immunohistochemical method were followed standard procedures (See Materials and Methods). Luminal epithelial cells (LE), myometrial cells (M), and glandular epithelial cells (GE), ×400. ATX, autotaxin.

LPA, a bioactive lipid signaling molecule (Hausmann et al., 2013; Magkrioti et al., 2023). LPA is a pleiotropic growth factor-like phospholipid, signaling via its G-protein coupled receptors (LPAR1-6) and activating a multitude of cellular signal transduction pathways (Magkrioti et al., 2019). Since ATX is profusely expressed in various cancer cell lines and its functions are related to cell proliferation and metastasis (Brindley, 2020), it can be expected that ATX may function in some tissues that show dynamic cell proliferation depending on physiological conditions, such as uterus or adipose tissue. Indeed, it has been reported that ATX and its receptor LPAR3 are expressed in the rat uterus, and their expressions are fluctuated during the reproductive cycle (Ahn et al., 2011). In human adipose tissue, visceral fat ATX expression was positively correlated with obesity (Rancoule

et al., 2012).

Mammalian uterus is dispensable organ for the survival of the individual, but it has a unique function of maintaining and raising offspring from implantation to birth through the placenta (Power & Schulkin, 2013; Roberts et al., 2016). To prepare for implantation of a fertilized egg while maintaining fertility, the uterus exhibits a reproductive cycle that repeats dynamic cell proliferation and death processes (Holdsworth-Carson et al., 2023; Hong, 2024). It is well known that the uterus is regulated by several specific steroid hormones as estrogen (E2) and progesterone (P4) in endometrium during uterus cycles (Martıín et al., 2002; Jang, 2018). Cumulative studies indicate the multi roles of ATX–LPA–LPAR signaling in uterus. LPAR3 is highly expressed in rodent uterine epithelium during the peri-implantation period, and has a critical role in the early pregnancy (Ye et al., 2005). Lpar3 KO mice exerted many reproductive defects, including significantly reduced cyclooxygenase-2 (COX-2), delayed implantation, aberrant embryo spacing, defects in placental formation and fetal development, and reduced litter size (Ye et al, 2005; Hama et al., 2006). In addition, up-regulation of heparin-binding (HB-) EGF and COX-2 in the uterine epithelium contributes to decidualization, and ATX–LPA–LPAR signaling at the embryo-epithelial boundary induces decidualization via the canonical HB-EGF and COX-2 pathways (Aikawa et al., 2017). ATX might participate in leiomyoma growth through local LPA formation via LPAR1 (Billon-Denis et al., 2008). In human endometrial stromal cells, through ATX-LPA1 signaling, LPA induces IL-8 expression via a nuclear factor-kappaB-dependent signal pathway, suggesting that LPA may play a role in angiogenesis of endometrium and placenta through induction of IL-8 in endometrial stromal cells during pregnancy (Chen et al., 2008). LPA with physiological concentrations could exert uterotonic effect via rat myometrial contraction (Nagashima et al., 2023). Taken together, these reports provide solid evidence on the crucial roles of ATX in the uterus in both normal and pregnant state. LPA, produced by ATX, may act as an autocrine and paracrine mediator of epithelial cell-to-epithelial cell and epithelial cell-to-stromal cell communication (Seo et al., 2008).

Concerning the estrous cycle, special attention should be given to the subdivision of the stages. Diestrus has the longest elapsed time and the serum hormone patterns in this stage show different aspects, we assume that subdividing this stage is more advantageous for accurately understanding the nature of reproductive cycle. We therefore refined the Diestrus stages as Metestrus and Diestrus; when the luteinization of granulosa cells are started at Metestrus, then corpus luteum formation begin, and progesterone level is increasing at Diestrus. In the present study, the uterine ATX expression was highest in Metestrus, decreased from Diestrus stage to Proestrus stage, and then increased in Estrus stage. In comparison, previous study divided the reproductive cycle into three stages, Proestrus-Estrus-Diestrus, and the authors observed the highest ATX expression at Diestrus, decreased expression at Proestrus, and the lowest expression at Estrus (Ahn et al., 2011). Combining these and our results, ATX expression at Metestrus (in other words, early Diestrus) is highest and begins to decrease as it progresses to the later Diestrus stage. Our immunohistochemical studies indicated that the strong positive signals were found in luminal epithelial cells, moderate signals were in myometrial cells, and weak signals in glandular epithelial cells in endometrium. In same cell type, the signals at Metestrus and/or Diestrus tend to be stronger than that at Proestrus and/or Estrus. Regarding the immunohistochemical studies, we believed that more careful approach, especially using sophisticated quantitative methods, will be needed.

With previous researches on the serum steroid levels during estrous cycle, the present study indicates that estradiol and progesterone may play crucial roles in the regulation of uterine ATX expression, since these two steroids are the lowest at the diestrus stage (Shaikh, 1971; de Greef & Zeilmaker, 1974; Ahn et al., 2011). Further studies on the ATX signaling–sex steroid relationship will be providing better understanding on the normal and pathophysiological state of uterus.

https://doi.org/10.12717/DR.2024.28.3.67

REFERENCES

Ahn HJ, Yang H, An BS, Choi KC, Jeung EB (2011) Expression and regulation of Enpp2 in rat uterus during the estrous cycle. J Vet Sci 12:379-385.

Aikawa S, Kano K, Inoue A, Wang J, Saigusa D, Nagamatsu T, Hirota Y, Fujii T, Tsuchiya S, Taketomi Y, Sugimoto Y, Murakami M, Arita M, Kurano M, Ikeda H, Yatomi Y, Chun J, Aoki J (2017) Autotaxin–lysophosphatidic acid–LPA_3 signaling at the embryo-epithelial boundary controls decidualization pathways. EMBO J 36:2146-2160.

Benesch MGK, Tang X, Maeda T, Ohhata A, Zhao YY, Kok BPC, Dewald J, Hitt M, Curtis JM, McMullen TPW, Brindley DN (2014) Inhibition of autotaxin delays breast tumor growth and lung metastasis in mice. FASEB J 28:2655-2666.

Billon-Denis E, Tanfin Z, Robin P (2008) Role of lysophosphatidic acid in the regulation of uterine leiomyoma cell proliferation by phospholipase D and autotaxin. J Lipid Res 49:295-307.

Brindley DN (2020) Lysophosphatidic acid signaling in cancer. Cancers 12:3791.

Chen SU, Lee H, Chang DY, Chou CH, Chang CY, Chao KH, Lin CW, Yang YS (2008) Lysophosphatidic acid mediates interleukin-8 expression in human endometrial stromal cells through its receptor and nuclear factor-κB-dependent pathway: A possible role in angiogenesis of endometrium and placenta. Endocrinology 149:5888-5896.

Choi JA, Kim H, Kwon H, Lee EH, Cho H, Chung JY, Kim JH (2023) Ascitic autotaxin as a potential prognostic, diagnostic, and therapeutic target for epithelial ovarian cancer. Br J Cancer 129:1184-1194.

de Greef WJ, Zeilmaker GH (1974) Blood pregesterone levels in pseudopregnant rats: Effects of partial removal of luteal tissue. Endocrinology 95:565-571.

Drosouni A, Panagopoulou M, Aidinis V, Chatzaki E (2022) Autotaxin in breast cancer: Role, epigenetic regulation and clinical implications. Cancers 14:5437.

Hama K, Aoki J, Bandoh K, Inoue A, Endo T, Amano T, Suzuki H, Arai H (2006) Lysophosphatidic receptor, LPA3, is positively and negatively regulated by progesterone and estrogen in the mouse uterus. Life Sci 79:1736-1740.

Hausmann J, Perrakis A, Moolenaar WH (2013) Structure–function relationships of autotaxin, a secreted lysophospholipase D. Adv Biol Regul 53:112-117.

Holdsworth-Carson SJ, Menkhorst E, Maybin JA, King A, Girling JE (2023) Cyclic processes in the uterine tubes, endometrium, myometrium, and cervix: Pathways and perturbations. Mol Hum Reprod 29:gaad012.

Hong IS (2024) Endometrial stem cells: Orchestrating dynamic regeneration of endometrium and their implications in diverse endometrial disorders. Int J Biol Sci 20:864-879.

Jang H (2018) Regulation of cyclic AMP-response element binding protein Zhangfei (CREBZF) expression by estrogen in mouse uterus. Dev Reprod 22(1):95-104.

Kanda H, Newton R, Klein R, Morita Y, Gunn MD, Rosen SD (2008) Autotaxin, an ectoenzyme that produces lysophosphatidic acid, promotes the entry of lymphocytes into secondary lymphoid organs. Nat Immunol 9:415-423.

Katsifa A, Kaffe E, Nikolaidou-Katsaridou N, Economides AN, Newbigging S, McKerlie C, Aidinis V (2015) The bulk of autotaxin activity is dispensable for adult mouse life. PLOS ONE 10:e0143083.

Kawagoe H, Soma O, Goji J, Nishimura N, Narita M, Inazawa J, Nakamura H, Sano K (1995) Molecular cloning and chromosomal assignment of the human brain-type phosphodiesterase I/nucleotide pyrophosphatase gene (PDNP2). Genomics 30:380-384.

Magkrioti C, Galaris A, Kanellopoulou P, Stylianaki EA, Kaffe E, Aidinis V (2019) Autotaxin and chronic inflammatory diseases. J Autoimmun 104:102327.

Magkrioti C, Kaffe E, Aidinis V (2023) The role of autotaxin and LPA signaling in embryonic development, pathophysiology and cancer. Int J Mol Sci 24:8325.

Martín J, Domínguez F, Ávila S, Castrillo JL, Remohí J, Pellicer A, Simón C (2002) Human endometrial receptivity: Gene regulation. J Reprod Immunol 55:131-139.

Mazzocca A, Schönauer LM, De Nola R, Lippolis A, Marrano T, Loverro M, Sabbà C, Di Naro E (2018) Autotaxin is a novel molecular identifier of type I endometrial cancer. Med Oncol 35:157.

Nagashima S, Kimura T, Terashima R, Sugiyama M, Kizaki K, Kawaminami M, Kurusu S (2023) Lysophosphatidic acid stimulates rat uterine contraction *in vitro*. J Reprod Dev 69:163-169.

Nakanaga K, Hama K, Aoki J (2010) Autotaxin: An LPA producing enzyme with diverse functions. J Biochem 148:13-24.

Nouh MAAM, Wu XX, Okazoe H, Tsunemori H, Haba R, Abou-Zeid AMM, Saleem MD, Inui M, Sugimoto M, Aoki J, Kakehi Y (2009) Expression of autotaxin and acylglycerol kinase in prostate cancer: Association with cancer development and progression. Cancer Sci 100:1631-1638.

Power ML, Schulkin J (2013) Maternal regulation of offspring development in mammals is an ancient adaptation tied to lactation. Appl Transl Genomics 2:55-63.

Rancoule C, Dusaulcy R, Tréguer K, Grès S, Guigné C, Quilliot D, Valet P, Saulnier-Blache JS (2012) Depot-specific regulation of autotaxin with obesity in human adipose tissue. J Physiol Biochem 68:635-644.

Roberts RM, Green JA, Schulz LC (2016) The evolution of the placenta. Reproduction 152:R179-R189.

Seo H, Kim M, Choi Y, Lee CK, Ka H (2008) Analysis of lysophosphatidic acid (LPA) receptor and LPA-induced endometrial prostaglandin-endoperoxide synthase 2 expression in the porcine uterus. Endocrinology 149:6166-6175.

Shaikh AA (1971) Estrone and estradiol levels in the ovarian venous blood from rats during the estrous cycle and pregnancy. Biol Reprod 5:297-307.

Stracke ML, Krutzsch HC, Unsworth EJ, Årestad A, Cioce V, Schiffmann E, Liotta LA (1992) Identification, purification, and partial sequence analysis of autotaxin, a novel motility-stimulating protein. J Biol Chem 267:2524-2529.

Umezu-Goto M, Kishi Y, Taira A, Hama K, Dohmae N, Takio K, Yamori T, Mills GB, Inoue K, Aoki J, Arai H (2002) Autotaxin has lysophospholipase D activity leading to tumor cell growth and motility by lysophosphatidic acid production. J Cell Biol 158:227-233.

Yang F, Chen GX (2018) Production of extracellular lysophosphatidic acid in the regulation of adipocyte functions and liver fibrosis. World J Gastroenterol 24:4132-4151.

Ye X, Hama K, Contos JJA, Anliker B, Inoue A, Skinner MK, Suzuki H, Amano T, Kennedy G, Arai H, Aoki J, Chun J (2005) LPA_3-mediated lysophosphatidic acid signalling in embryo implantation and spacing. Nature 435:104-108.

Zeng Y, Kakehi Y, Nouh MAAM, Tsunemori H, Sugimoto M, Wu XX (2009) Gene expression profiles of lysophosphatidic acid-related molecules in the prostate: Relevance to prostate cancer and benign hyperplasia. Prostate 69:283-292.

Zhang X, Li M, Yin N, Zhang J (2021) The expression regulation and biological function of autotaxin. Cells 10:939.

https://doi.org/10.12717/DR.2024.28.3.67